KONINKLIJK NEDERLANDS METEOROLOGISCH INSTITUUT

WETENSCHAPPELIJK RAPPORT
SCIENTIFIC REPORT

W.R. 80 - 4

W. Kohsiek and W.A.A. Monna

A fast response psychrometer.

De Bilt 1980

Publikatienummer: K. N. M. I. W. R. 80 - 4 (M. O.)

Koninklijk Nederlands Meteorologisch Instituut,
Meteorologisch Onderzoek,
Postbus 201,
3730 AE De Bilt,
Nederland.

U.D.C.: 551.508.71

Abstract

A fast thermocouple psychrometer is described. The sensors, which are constructed from head-on welded chromel-alumel junctions of 50 μm diameter wire, are mounted vertically. The wick is a fine polyester thread covering the thermocouple wires over a length of about 20 mm. The wet junction is supplied with water by droplets falling along the wick with a frequency of about one per minute.

The falling drop method ensures a reliable wetting of the wet bulb. Moreover, accumulation of dirt on the wick is avoided. The response times of the wet bulb and the dry bulb have been measured by means of wind tunnel experiments. At a wind speed of 4 m s^{-1} the response time of the wet bulb is 0.3 s, that of the dry bulb is 0.05 s. A study has been made of several possible error sources. The effect of radiation is a few tenths of a degree Celsius for both bulbs. The wet bulb may be influenced by electrochemical voltages unless deionized or destillated water is used. The instrument has been used with several measuring campaigns and proved to work reliably.

-o-o-o-

Contents

1. Introduction

The Royal Netherlands Meteorological Institute is carrying out a research programme on the atmospheric boundary layer. For that purpose a 213 m high meteorological tower was erected near the village of Cabauw. Among many other quantities the sensible heat flux is measured at heights between 20 and 200 m with the eddy correlation technique (Van Ulden et al., 1976; Driedonks et al., 1978). This technique is based on the simultaneous measurement of fluctuations of the vertical wind speed and fluctuations of the transported quantity, in this case temperature. The frequencies of the fluctuations that are to be detected depend on the height of observation. As a rule of thumb, the highest frequency of importance is about twenty times the inverse of the observation height (e.g. 1 Hz at 20 m), the lowest frequency is about 0.001 Hz.

The research programme will be extended in the near future with the study of water vapour transport in the boundary layer. For the measurement of water vapour flux a fast psychrometer has been developed. This instrument is subject of the present report.

We opted for a thermocouple psychrometer because such an instrument is relatively easy to construct, simply to operate, and it has a stable calibration (in contrast to e.g. optical absorption methods). Various psychrometers for eddy correlation measurements have been reported in the literature. Far from trying to be complete, we mention the hygrometer used in the so-called evapotron of Dyer and Maher (1965), which employs resistance thermometers, the psychrometer of Polavarapu (1972) with copper-constantan thermocouples, and the instrument described by Tillman (1973), which uses chromel-constantan thermocouples and an active electronic circuit to extend the high frequency range. Quoted time constants for the wet bulb are in the range of 0.1-0.5 s. The dry bulbs are usually much faster. A common

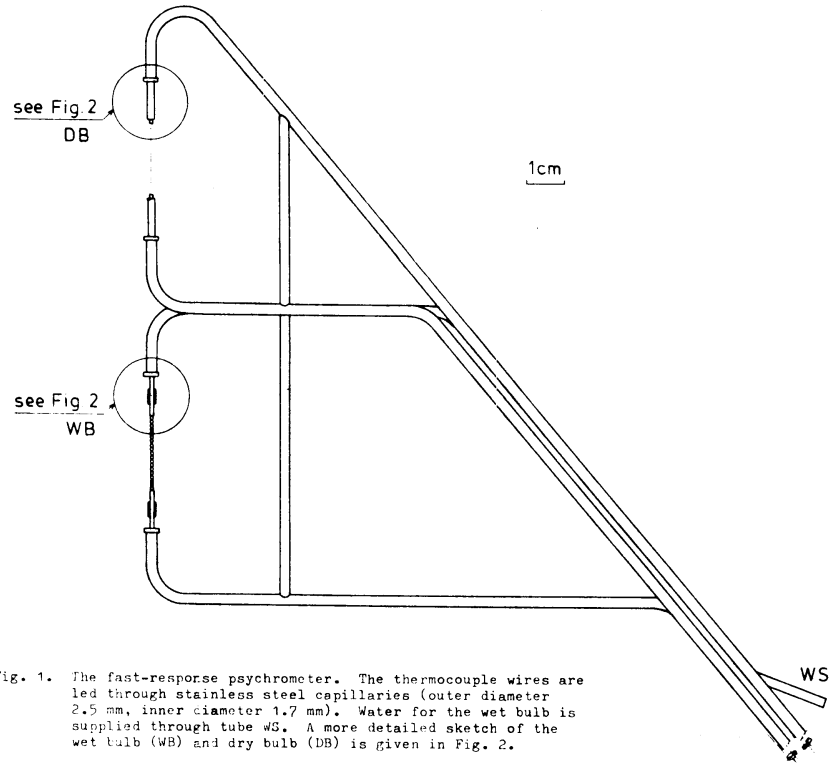

Fig. 1. The fast-response psychrometer. The thermocouple wires are led through stainless steel capillaries (outer diameter 2.5 mm, inner diameter 1.7 mm). Water for the wet bulb is supplied through tube WS. A more detailed sketch of the wet bulb (WB) and dry bulb (DB) is given in Fig. 2.

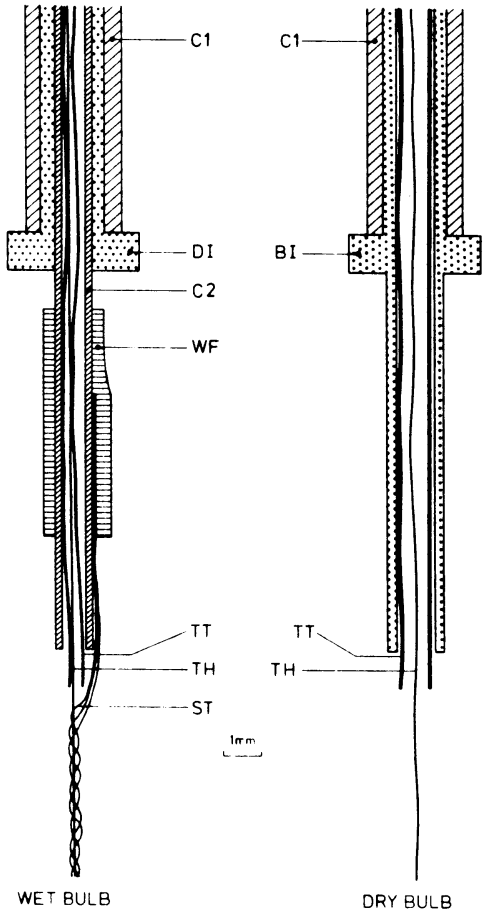

Fig. 2. Construction of the wet-bulb and dry-bulb element. Wet bulb: C_1 is the stainless steel capillary of the housing. C_2 is a smaller stainless steel capillary (outer diameter 1 mm, inner diameter 0.64 mm), which is mounted in the housing by means of an insulating Delrin plug DI. (The thermocouple wire (TH) is insulated by means of a teflon tube (outer diameter 0.29 mm, inner diameter 0.08 mm). Water is transported in the space between the capillary C_2 and the teflon tube. The 3-strand polyester wire (ST) is clamped under a piece of silicon tubing WF. Dry bulb: The housing capillary C_1 is extended by a smaller, chromium plated brass capillary BI. The thermocouple wire is insulated by a teflon tube TT with outer diameter 0.9 mm and inner diameter 0.7 mm.

practical problem with these instruments is the water supply to the wet bulb. The instrument we designed has a reliable water supply.

The construction of our psychrometer is described in section 2 of this report. The next section deals with several physical aspects of the sensor: the theoretical response times of the dry bulb and the wet bulb, the internal response times of the bulbs, and a few phenomena which may influence the sensor's output erroneously, such as heat conduction along the thermocouple wires, galvanic leak currents, and radiation. Section 4 deals with calibrations: the thermocouple voltage as a function of temperature, observed response times and the psychrometer constant. In section 5 a few notes are given on practical experiences with the psychrometer. The report is concluded with an appendix listing some properties of chromel and alumel, and an appendix on the mathematical derivation of the internal response times of the dry bulb and the wet bulb.

2. Description of the sensor

Figures 1 and 2 show the sensor design. The 50 μm thermocouple wires are led through stainless steel capillary tubes (inner diameter 1.7 mm, outer diameter 2.5 mm). About 2 cm wire, with the thermocouple in the middle, is free to the atmosphere. The whole array can be mounted on an electrical connector. In the following some details of the construction are discussed.

Chromel and alumel thermocouples were chosen for the following reasons: easy to weld, low thermal conductivity (stem error), rather high thermo e.m.f. (about 40 μV/°C). (For a summary of some material constants of the metals, see Appendix I). The wires are not insulated, because removal of insulation, necessary for the welding process, offered difficulties (damaging of the wires). Afterwards, the wires have been insulated for the greater part by teflon tubes of 0.9 mm

outer diameter and 0.1 mm wall thickness. As for the wet-bulb sensor, the last few centimeters of wire before leaving the short capillary tubes have been insulated by teflon tube of 0.29 mm outer diameter and 0.08 mm wall thickness. (See Fig. 2). The outer diameter of the short stainless steel capillaries, 1 mm, is chosen empirically on the basis of the optimum size of the water drops formed at the exit of the upper capillary. The inner diameter is 0.64 mm.

The head-on welds of the thermocouple wires were made by the Technical and Physical Engineering Research Service at Wageningen, The Netherlands. The shape of the weld is more or less an ellipsoid with a thickness of about twice the diameter of the wires. It is important that the junction has a smooth surface, otherwise the mounting of the wick offers difficulties afterwards. The cold junction is mounted together with a thermistor in a small aluminium cylinder situated near the connector. The signal of the thermistor is electronically translated into a thermocouple signal with its cold junction at 0 ^{o}C, and added to the signals of the dry bulb and the wet bulb. There are no other junctions in the thermocouple wires, because otherwise extra thermo voltages might be generated (junctions between wires of the same material but with different diameters may exhibit considerable thermo e.m.f.'s).

To moisten the wet bulb, a fine polyester thread, made up of three strands, is wound around the part of the thermocouple wires that is exposed to the atmosphere, in such a way that the original winding structure of the thread is not lost (Fig. 2). This results in an overall diameter of about 0.3 mm. Water is supplied from above, through the same capillaries where the thermocouple wire is led through. The water supply is forced by a peristaltic pump. At the end of the short capillary a drop is formed, which eventually detaches and falls along the wick. By this process a faultless wetting of the wet bulb is ensured, even under the most dry air conditions. One only has to take care that the wick is wetted in some other

way at the onset of an experiment, because the dripping process may not always succeed in wetting a dry wick. The drip frequency we used is about twice per minute. This method of moistening the wet bulb has the additional advantage that it keeps the wick free from dirt.

The electronics may be placed at tens of meters from the sensor. Its function is to amplify the thermo e.m.f.'s of the dry and the wet bulb, and to transform the resistance of the thermistor into an equivalent thermocouple signal. The response time of the electronics is about 50 ms. The output voltages are on 10 V level, compatible to commonly used digital sampling systems. Since all metal parts are connected to ground potential, the whole sensor system is protected against h.f. interference.

3. Physical properties of the sensor

3.1 Theoretical response time

The sensing element is assumed to be a massive cylinder with a uniform temperature and negligible heat transport at the ends. The heat transferred to the cylinder is stored in it. For the dry bulb:

$$\alpha A(T - T_d) = -C \frac{dT}{dt} \quad , \tag{1}$$

where T is the temperature of the cylinder, T_d that of the ambient air at some distance from the cylinder, α the heat transfer coefficient, A the area of the cylinder and C its heat capacity; t is the time.

Since

$$C = \rho_c c_{pc} V = \rho_c c_{pc} \frac{R}{2} A \tag{2}$$

with ρ_c the density of the cylinder, c_{pc} its specific heat capacity, V its volume and R its radius, (1) can also be written like:

$$\frac{dT}{dt} + \frac{2\alpha}{\rho_c c_{pc} R} (T - T_d) = 0 \quad . \tag{3}$$

From this differential equation follows the response time constant τ_d :

$$\tau_d = \frac{\rho_c c_{pc} R}{2\alpha} \quad . \tag{4}$$

For the wet bulb, the heat transfer by evaporation has also to be considered. The energy budget equation is:

$$\alpha A(T - T_d) + \beta A[\rho_{vs}(T) - \rho_v] = -C_w \frac{dT}{dt} \quad , \tag{5}$$

where ρ_v is the ambient absolute humidity (kg m^{-3}), $\rho_{vs}(T)$ the saturated absolute humidity at temperature T and β the water vapour transfer coefficient. C_w is the heat capacity of the wet bulb. If heat and water vapour are transferred in a turbulent air flow, we can write in good approximation (Wylie, 1968a; Monteith, 1973):

$$\alpha/\beta = \rho c_p/L \overset{\text{def}}{=} \gamma \quad , \tag{6}$$

where ρ is the density of dry air and c_p its specific heat capacity, and L the heat of evaporation of water. Note that the dimensions of α and β are different. The quantity γ (dimension: kg (water)/m^3 K) may be called the psychrometer coefficient (The psychrometer <u>constant</u> is a pressure-"corrected" quantity with dimension K^{-1}, see Wylie, 1968c). Eq. (5) can now be rewritten as

$$\alpha A(T - T_d) + \frac{\alpha}{\gamma}[\rho_{vs}(T) - \rho_v] = -C_w \frac{dT}{dt} \quad . \tag{7}$$

In equilibrium state (dT/dt = 0) the wet-bulb temperature (T_w) is implicitly given by

$$\rho_v = \rho_{vs}(T_w) - \gamma \cdot (T_d - T_w) \quad . \tag{8}$$

Next, using (8), we make the following approximation:

$$\rho_{vs}(T) - \rho_v = \rho_{vs}(T) - \rho_{vs}(T_w) + \rho_{vs}(T_w) - \rho_v =$$

$$\approx s(T - T_w) + \gamma(T_d - T_w) \quad , \tag{9}$$

where $s = (d\rho_{vs}/dT)$ at $T = (T_w + T)/2$ is the slope of the saturated absolute humidity versus temperature curve. From (7) and (9) follows:

$$\alpha A \left[(T - T_d) + \frac{s}{\gamma} (T - T_w) + (T_d - T_w) \right] = -C_w \frac{dT}{dt} \tag{10}$$

or: $$\frac{dT}{dt} + \frac{2\alpha}{\rho_w c_{pw} R} \left(1 + \frac{s}{\gamma}\right) (T_c - T_w) = 0 \quad , \tag{11}$$

Here, $\tau_w c_{pw}$ is the heat capacity per unit volume of the wet bulb, and R its radius. So the time constant τ_w for the wet bulb is:

$$\tau_w = \frac{\rho_c c_{pc} R}{2\alpha} \frac{1}{1 + s/\gamma} \quad . \tag{12}$$

The heat transfer coefficient α for a cylinder with diameter d may be expressed as (Monteith, 1973):

$$\alpha = Nu \frac{k}{d} \quad , \tag{13}$$

where Nu is the Nusselt number and k the thermal conductivity of air. The Nusselt number is a function of the Reynolds number $Re = ud/\nu$, where u is the wind velocity and ν the kinematic viscosity of air. Usually the relations are of the type

$$Nu = K_1 Re^{K_2} \tag{14}$$

where the empirical constants K_1 and K_2 may be chosen differently for different intervals of Re. In our case, the Reynolds numbers are in the range 4-400. Following Monteith (1973) we put:

$$\begin{aligned} Nu &= 0.82\ Re^{0.39} \qquad 4 < Re \leqslant 40 \\ Nu &= 0.62\ Re^{0.47} \qquad Re > 40\ . \end{aligned} \tag{15}$$

Now, we can calculate the time constants τ_d and τ_w. For example:

dry bulb $\rho_c c_{pc} = 4 \times 10^6$ J m^{-3} K^{-1} (Nickel)

$R = 25\ \mu m$

$u = 4$ m s^{-1} $\rightarrow$ Nu = 228, $\alpha = 1150$ W m^{-2} K^{-1}

$\tau_d = .043$ s

wet bulb $\rho_w c_{pw} = 4.2 \times 10^6$ J m^{-3} K^{-1} (water)

$R = 150\ \mu m$

$u = 4$ m s^{-1} $\rightarrow$ Nu = 4.92, $\alpha = 415$ W m^{-2} K^{-1}

$\gamma(s+\gamma) = 0.37$ (at 15 °C)

$\tau_w = .28$ s

In these calculations we used $k = 25.3 \times 10^{-3}$ W $m^{-1}K^{-1}$ and $\nu = 1.46 \times 10^{-5}$ m^2 s^{-1}. It is assumed that the heat capacity per unit volume of chromel and alumel is that of nickel, which forms the main constituent of both the alloys (see Appendix I). The wet bulb is made up of thermocouple wire, water and the wick. Because the heat capacities per unit volume of water and nickel differ only by 5 % and water makes up about 97 % of the volume of the wet bulb, we assumed that the heat capacity per unit volume of the whole assembly is that of water.

3.2 Heat conduction errors

The dry bulb.

The temperature of the thermocouple junction may be influenced by heat conduction along the thermocouple wires. With our design, the nearest places where the thermocouple wire may be forced to assume a temperature different from the air temperature are the places where the wire enters the teflon tubes, at about 1 cm from the junction (Fig. 2). The effect on the temperature of the junction can be predicted with a sample model: we schematize the problem to that of a homogeneous cylinder, placed in an air flow with temperature T_d, having a temperature T_e at its end points. The length of the cylinder is 2e. The equilibrium state is described by equality of radial heat transport and axial heat divergence:

$$\alpha \cdot 2\pi R(T - T_d) = \lambda \pi R^2 \frac{d^2T}{dx^2} \quad , \tag{16}$$

where λ is the coefficient of heat conduction of the cylinder and x the axial coordinate (the middle of the cylinder is at $x = 0$). As radial temperature gradients have been neglected, (16) holds strictly speaking only at some distance (a few times the wire diameter) from the end point of the cylinder. The boundary conditions to (16) are:

$$T = T_e \quad \text{at} \quad x = \pm e$$

$$dT/dx = 0 \quad \text{at} \quad x = 0. \tag{17}$$

The solution of (16) with (17) is:

$$T(x) = T_d + (T_d - T_e) \frac{\cosh px}{\cosh pe} \quad , \tag{18}$$

where $p = (2\alpha/\lambda R)^{\frac{1}{2}}$. The temperature error at $x = 0$ is consequently:

$$T(0) - T_d = (T_e - T_d) \cosh pe \; . \tag{19}$$

For numerical evaluation, the highest thermal conductivity of the two metals alumel and chromel is adopted (alumel, $\lambda = 28$ W $m^{-1}K^{-1}$, see Appendix I), $R = 25$ μm, $e = 10^{-2}$ and $\alpha = 1150$ W $m^{-2}K^{-1}$ (wind speed 4 m s^{-1}, see foregoing section). The temperature difference $T_e - T_d$ is assumed to be 10 °C (this is an over-estimation). With these values, the temperature error is:

$$T(0) - T_d = 10/\cosh 18.1 = 2.8 \times 10^{-7} \text{ °C}$$

which indicates that the effect is negligible. The distance e for which the temperature error is 0.01 °C, which is regarded as the ultimately tolerable, is also of interest; it follows from:

$$\cosh(1810\ e) = 10/10^{-2} \rightarrow e = 4.2 \times 10^{-3} \text{ m}.$$

The wet bulb.

The geometry of the wet bulb may be schematized to a small cylinder (thermocouple wire), embedded in a larger one (the wick). The effective heat conductivity is in first approximation the sum of the heat conductivities of the metal and water, weighted by their relative cross-sections:

$$\lambda_{eff} = \lambda_m \left(\frac{R_c}{R_w}\right)^2 + \lambda_{H_2O} \left[1 - \left(\frac{R_c}{R_w}\right)^2\right], \qquad (20)$$

where R_c is the radius of the thermocouple wire and R_w that of the outer water surface. With $R_c = 25$ μm, $R_w = 150$ μm, $\lambda_m = 28$ W $m^{-1}K^{-1}$ and $\lambda_{H_2O} = 0.6$ W $m^{-1}K^{-1}$, the effective heat conduction is:

$$\lambda_{eff} = 28 \times \frac{1}{36} + 0.6 \times \frac{35}{36} = 1.36 \text{ W } m^{-1}K^{-1}.$$

The equivalent to (16) for the wet bulb is:

$$\alpha\left(1 + \frac{s}{\gamma}\right) 2\pi R(T - T_w) = \lambda_{eff}\ \pi R^2 \frac{d^2T}{dx^2}. \qquad (21)$$

Here, the factor $(1 + s/\gamma)$ reflects that both sensible and latent heat transports take part in the process. This factor can be derived in the same way as is done for the response time, see (11). The boundary conditions are the same as for the dry bulb, Eq. (17). So the temperature error is:

$$T(0) - T_w = \frac{T_e - T_w}{\cosh pe} \quad , \tag{22}$$

analogous to (19). Here, $p = [\, 2\alpha (1 + s/\gamma)/\lambda_{eff} R \,]^{\frac{1}{2}}$. With $\lambda_{eff} = 1.36$ W $m^{-1}K^{-1}$, $R = 150$ μm, $\alpha = 415$ W $m^{-2}K^{-1}$ (wind speed 4 m s^{-1}) and $(1 + s/\gamma) = 2.7$ (at 15 °C), the value of p is 3.31×10^3 m^{-1}. This is considerably smaller than in the foregoing example for the dry bulb (p (dry bulb) = 1.81×10^3 m^{-1}). The temperature of the cylinder at about 1 cm from the middle may be forced to assume the temperature of the metal capillary, because there water droplets provide a good thermal contact. Assuming $T_e - T_w = 20$ °C, and $e = 10^{-2}$ m, the wet-bulb temperature error is:

$$T(0) - T_w = 20/\cosh 33.1 = 1.7 \times 10^{-13} \ ^{\circ}C.$$

So the effect of heat conduction along the sensor is also for the wet bulb negligible. The distance e for which the temperature error is 0.01 °C follows from:

$$\cosh (3310\, e) = 20/10^{-2} \rightarrow e = 2.5 \times 10^{-3} \text{ m}.$$

Conclusion: it is not to be expected that the dry-bulb and wet-bulb temperatures measured with the device are affected by heat conduction along the sensing elements.

3.3 Internal response time of the sensors

We consider a homogeneous cylinder at uniform temperature. At time $t = 0$ the temperature of the wall of the cylinder is stepwise decreased by an amount ΔT. We consider the temperature response of the cylinder. The internal heat transport is described by:

$$\frac{\partial T}{\partial r} = \kappa \frac{1}{r} \frac{\partial}{\partial r} \left(r \frac{\partial T}{\partial r} \right) , \tag{23}$$

where κ is the thermal diffusivity, $\kappa = \lambda / \rho_c c_{pc}$. The boundary conditions are:

$$\begin{aligned} T(r,t) &= \Delta T \qquad 0 \leqslant r < R \ , \ t = 0 \\ T(R,0) &= 0. \end{aligned} \tag{24}$$

The solution of (23), (24) is (see Appendix II):

$$T(r,k) = 2\Delta T \sum_{n=1}^{\infty} \frac{J_0(j_{on} r/R)}{j_{on} J_1(j_{on})} \exp\{- \kappa j_{on}^2 t/R^2\} \ , \tag{25}$$

where J_0 and J_1 are Bessel functions of the order 0 and 1 respectively, and j_{on} is the n^{th} zero of J_0. In case of the dry bulb, one is interested in the average temperature of the cylinder ($\overline{T(t)}$):

$$\overline{T(t)} = \int_0^R \frac{2\pi r}{\pi R^2} T(r,t) dr = 2 \int_0^1 \frac{r}{R} T(r,t) \, d \frac{r}{R} =$$

$$= 4\Delta T \sum_{n=1}^{\infty} \int_0^1 \frac{r}{R} \frac{J_0(j_{on} r/R)}{j_{on} J_1(j_{on})} \exp\{ - \kappa j_{on}^2 t/R^2 \} \, d \frac{r}{R} =$$

$$= 4\Delta T \sum_{n=1}^{\infty} \frac{1}{j_{on}^2} \exp\{ - \kappa j_{on}^2 t/R^2 \} . \tag{26}$$

Here the relation $\int_0^1 p \, J_0(j_{on} p) dp = J_1(j_{on})/j_{on}$ has been used (see e.g. Burkill, 1962).

Now, let us suppose that the system would behave like a first-order system with a time constant $\tau_{int,dry}$. At this moment of time the right-hand side of (24) would have the value $\Delta T/e$. So:

$$1/e = 4 \sum_{n=1}^{\infty} \frac{1}{j_{on}^2} \exp\{ - \kappa j_{on}^2 \tau_{int,dry}/R^2 \} \quad . \qquad (27)$$

It is found that:

$$\tau_{int,dry} = 0.11 \, R^2/\kappa \quad . \qquad (28)$$

As it turns out that the first term in the series (27) is dominating (the second is 1.3 % of the first, the third 38×10^{-3} %), so for $t \gtrsim \tau_{int,dry}$ the system behaves indeed like a first-order one. The numerical value of $\tau_{int,dry}$ is, with $\kappa = 4.5 \times 10^{-6}$ $m^2 s^{-1}$ (chromel) and $R = 25$ µm, 0.015 ms, much less than the external response time (of the order of 40 ms).

For the wet bulb, the temperature in the centre of the water cylinder, where the thermocouple wires are situated, is of interest. (It is supposed that the metal core has a negligible effect on the internal response characteristics, because its response time is much less than that of the water cylinder). So:

$$T(0,t) = 2\Delta T \sum_{n=1}^{\infty} \frac{1}{j_{on} J_1(j_{on})} \exp\{- \kappa j_{on}^2 \, t/R^2\} \quad . \qquad (29)$$

The same reasoning as before for the dry bulb leads to:

$$\tau_{int,wet} = 0.25 \, R^2/\kappa \quad . \qquad (30)$$

Again, the first term dominates by far, so the internal wet bulb behaves also like a first-order system for $\tau \gtrsim \tau_{int,wet}$. With $R = 150$ µm and $\kappa = 0.143 \times 10^{-6}$ $m^2 s^{-1}$ (water), $\tau_{int,wet} = 0.039$ s, again short compared with the external response time (order of 0.30 s).

The conclusion is that, for temperature fluctuation frequencies of practical interest, one can assume the dry-bulb and the wet-bulb elements to be isothermal.

3.4 Effect of galvanic voltages (wet bulb)

The water needed to wet the wet-bulb element will also act like a galvanic element with an electromotive force. The internal resistance of the electrolyte depends heavily on the purity of the water used. Two effects are to be considered (see Fig. 3):

(a) the e.m.f. generated in the immediate neighbourhood of the thermocouple junction;

(b) the e.m.f. generated between the thermocouple wires and the stainless steel support.

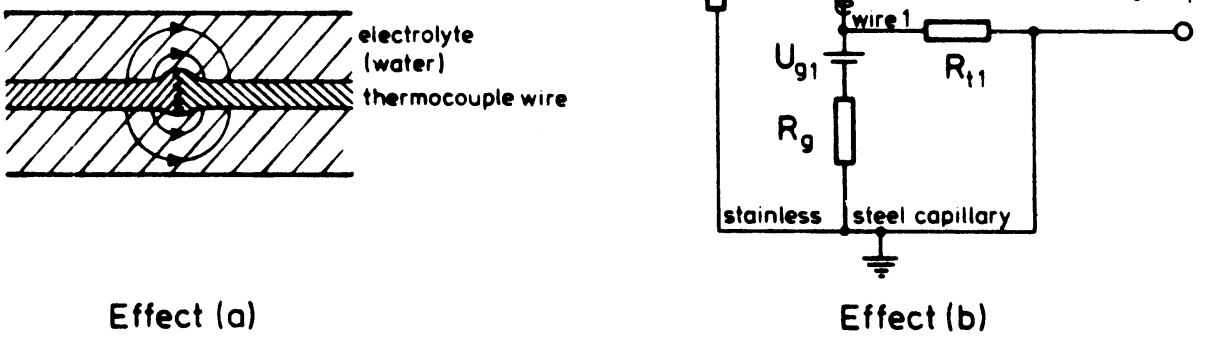

Fig. 3. Schema of the possible galvanic effects. U_{g1}, U_{g2}: galvanic voltages; R_g: internal resistance of the galvanic element; R_{t1}, R_{t2}: resistances of the thermocouple wires; Z_i: input impedance amplifier.

Effect (a)

In the immediate neighbourhood of the junction a galvanic voltage is generated due to difference of the contact potentials water/chromel and water/alumel, which is of the order of 0.1 V. We investigated the effect experimentally by constructing a chain of a wet-bulb and dry-bulb element, placed in a thermal isolated, closed box, which was partially filled with water;

the wet element was supplied with the liquid by capillary transport. The e.m.f. generated in the chain is measured. After several hours, the air inside the box is saturated with water vapour, and a possibly observed e.m.f. can only have been generated by galvanic effects, because the wet-bulb and dry-bulb element have the same temperature. We did not find any effect exceeding a few tenths of a microvolt, whether we used pure water, tap water or a solution of 0.5 % H_2SO_4 and 1 % $CuSO_4$ in water. From these results we concluded that effect (a) may be ignored.

Effect(b)

Due to the electromotive force U_{g2} of the galvanic element thermocouple wire-electrolyte-stainless steel capillary, an electric current runs through thermocouple wire 1, and generates a potential difference over the wire (resistance R_{t1}). The same holds for U_{g1}. The extra voltage observed over the end points of the thermocouple wires is:

$$U_g = \frac{U_{g2} R_{t1}}{R_g + R_{t1}} + \frac{U_{g1} R_t}{R_g + R_{t2}} \quad . \qquad (31)$$

In (31) we assumed equal internal resistances for the electrolytes The electromotive forces U_{g1} and U_{g2} were found to be about 0.2 V. The resistance R_e was found by measuring the resistance between the thermocouple wires and the stainless steel capillaries. A value of the order of 20 MΩ was observed using deionized water, 5 MΩ in case of tap water and 200 KΩ for a solution of 15 g NaCl in 500 g water. Assuming $U_{g1} = U_{g2}$, and using the inequality $R_{t1}, R_{t2} \ll R_g$, (31) reduces to:

$$U_g = 2 \frac{U_{g1}}{R_g} R_{t1} \quad . \qquad (32)$$

With our design, the chromel wire is connected with earth potential. Then, $R_{t1} = 90\,\Omega$. Using deionized water, the extra voltage is:

$$U_g = 2 \times \frac{0.2}{2 \times 10^7} \times 90 = 1.8 \times 10^{-6} \text{ V.}$$

This corresponds to a temperature error of about 0.05 °C. With the salt solution, an error of several degrees Celsius is expected. An error of this magnitude was indeed observed. So effect (b) may only be neglected if deionized water is used. This condition is not always easily to meet in practice. The effect may be avoided by decoupling the electronic amplifier from the sensor frame. Also, reducing the resistance of the thermocouple leads (R_{t1} and R_{t2}) may eliminate the effect. However, this solution requires wires with larger diameters than those of the external ports, and consequently introduces extra junctions, which may generate extra thermo e.m.f.'s. Finally, it should be remarked that a galvanic off-set does not affect the performance of the instrument as a temperature fluctuation sensor, as long as the variation of the off-set is much less than that of the phenomenon to be observed.

3.5 Effect of radiation

The temperature of the thermocouple junctions may be influenced by radiative processes. In the following we will treat shortwave and longwave effects separately.

Shortwave radiation effect.

Let us assume that shortwave radiation with an irradiance of $E(W\ m^{-2})$ is incident on the surface of the sensing element that has an absorption coefficient a. Let us further assume that the radiation is isotropic; this is a rather crude approximation. We are, however, only interested in the order of magnitude of the radiation effect, not in its exact value (which in practice will depend on the contributions of direct and diffuse solar radiation, sun height, surface albedo, etc.). Then the element absorbs per unit of area $aE\ (W\ m^{-2})$. As a result, the temperature of the element will rise to a new equilibrium state

in which the radiative heat gain is balanced by heat loss to the air; in formula:

$$aE = \alpha (T - T_d) \qquad \text{(dry bulb)}$$
$$aE = \alpha (1 + s/\gamma)(T - T_w) \qquad \text{(wet bulb)} . \qquad (33)$$

Here, T is the equilibrium temperature with radiation, T_d is the air temperature and T_w the wet-bulb temperature. The absorption coefficient a is estimated at 0.3 for the wet bulb: the wick is made up of white tissue, which darkens in the course of time due to pollution. For the dry bulb the estimate is 0.5: if new, the thermocouple wires are reflecting, but the reflection diminishes; the junction itself is rather dark. An upper estimate for E is 800 W m^{-2}. The heat exchange coefficient α is 1152 W $m^{-2}K^{-1}$ for the dry bulb, and 415 W $m^{-2}K^{-1}$ for the wet bulb (wind speed 4 m s^{-1}; see section 3.1). The factor $1 + s/\gamma$ has the value 2.7 at 15 °C. For these parameters, the radiation temperature errors are:

$$T - T_d = 0.35\ ^{o}C \qquad \text{(dry bulb)}$$
$$T - T_w = 0.21\ ^{o}C \qquad \text{(wet bulb)}.$$

The phenomenon was also observed experimentally by shading the sensors from direct sunlight by the hand. A temperature effect of 0.1-0.2 °C was found for both the dry- and the wet-bulb sensor.

Longwave radiation effect.

The sensors exchange longwave radiation with their surroundings. If the temperature of the surroundings is different from that of the sensor, a net radiative heat transport will take place. The magnitude of this transport depends on temperature differences, and the (longwave) absorption coefficient of the sensors. We will make an estimation of the maximum effect, and therefore put the absorption coefficients equal to 1. The surroundings may be divided into two hemispheres: the earth and the sky. At night, both hemispheres may be lower in temperature

than the air temperature, and a maximum effect for the dry bulb is to be expected. We assume the earth temperature to be by 10 °C lower than the air temperature (clear night, vegetated surface), and the effective sky temperature by 20 °C lower (cloudless sky, low humidity). The net radiative transport per unit of area is in that case about 80 W m^{-2}, and the resulting temperature error (with the same heat exchange coefficients as used above for the shortwave effect) is -0.07 °C. For the wet bulb, the effect may be less because the sensor temperature is lower than the air temperature. By day, the actions of the warm earth surface and the cold sky may compensate each other for the dry bulb, but not for the wet bulb. Anyhow, the effect on both errors is expected to be not more than 0.1 °C.

Summarizing, the short wave radiation effect on the temperature of the sensors is found to be in the order of a few tenths of a degree Celsius. This may influence the performance of the sensors as temperature fluctuation detectors in case of rapid changing irradiance, e.g. a partly clouded sky. The effect of longwave radiation is less than 0.1 °C.

3.6 Effect of the water supply

Deionized water is supplied to the sensor by a peristaltic pump at a rate of about two droplets per minute. This ensures that the tissue remains wet even under the most unfavourable condituins (dry air, high wind speed). Each time a drop of water is passing the thermocouple junction, the temperature of the junction is disturbed, because the temperature of the drop is generally somewhat higher than the wet bulb temperature. The disturbance is found to be in the order of a few tenths of a degree Celsius. The characteristic time for the effect is the sensor's response time. These disturbances will lead to an extra temperature variance, which can be estimated as follows:

Let us assume a response time of .3 s (section 4.2), a temperature disturbance of .3 °C, and a droplet frequency of 1/30 s^{-1}. Then, if one takes many instantaneous samples of the temperature

during a time interval much longer than 30 s, one out of a hundred samples will be taken during the disturbed situation. The variance, occasioned by this effect is:

$$\frac{1}{99}\,(0.3^2 \times 1 + 0^2 \times 99) \approx 0.001\ {}^{o}C^2.$$

Temperature variances observed in the neutral or unstable atmosphere are of the order of 0.1 $^{o}C^2$ or higher. So the contribution of the water drops to the variance is negligible, unless a very stable atmosphere is studied where the temperature variance may be much lower than 0.1 $^{o}C^2$. The effect on heat flux measurements is expected to be nil for all situations, because there is no correlation between the disturbances of the droplets and the vertical wind velocity.

In practice, we used two sensors in series. This doubles the frequency of the disturbances, but halves the temperature effect. The variance is than half the one calculated above.

4. Calibrations

4.1 Calibration of the thermocouple

The chromel alumel thermocouple was calibrated with a platinum resistor as a standard. One junction was kept at 0 ^{o}C in a Mectron Geref Ice-Point Reference Unit, whilst the other junction was immersed in benzine, together with the Platinum resistor. A Dewar jar was used to keep the temperature of the benzine as constant as possible. To avoid temperature gradients, the benzine was stirred continuously by a motor-driven propeller. Copper wire was used to connect the thermocouple with a Hewlett Packard 3420B compensating voltmeter. The two copper junctions were placed in an aluminium cube, to keep them at the same temperature. The platinum resistor was connected with a Data Precision 1455 multimeter.

So a 13-point calibration between -25 °C and +35 °C was carried out. The relation between the thermocouple output U(μV) and the temperature T (°C) was found to be

$$U = 38.75\ T + 0.0275\ T^2 - 0.86 \qquad (34)$$

The absolute accuracy of this calibration is 0.1 °C.

4.2 Determination of the time constants

The time constants of the wet and the dry thermocouple depend on the wind speed; so measurements were carried out in the wind tunnel of the Royal Netherlands Meteorological Institute (KNMI) at De Bilt. This tunnel is of the open Eiffel-type with closed instrument compartment, which measures 0.4 x 0.4 x 0.4 m.

The temperature of the thermocouples was raised to some degrees above equilibrium by radiation. For that purpose the beam of light from a slide projector, placed outside the wind tunnel, was focussed on the thermocouple. Next, the beam of light was cut off by a slide and while the thermocouple regained the equilibrium temperature, its electrical output was amplified and registrated on a Hewlett Packard 181A memory oscilloscope. The signal was found to be exponential for over one decade. In this way the time constant of the thermocouple was determined for various wind speeds. The interruption time of the beam was 10 ms. At high wind speeds the time constant of the dry thermocouple is so small that there may be some influence of the interruption time on the measured time constant. Finally, it should be mentioned that for the wet-bulb measurements a mirror was used to realize a more uniform heating of the thermocouple. (However, no effect of the mirror on the measured values of both thr wet-and dry-bulb time constants could be found).

The values of the time constants τ_d (dry bulb) and τ_w (wet bulb) as a function of the wind speed u are given in Table 1.

Table 1. Time constants (ms) as functions of wind speed u (ms).

	observed	theoretical	
τ_d	$87\ u^{-0.35}$	$75\ u^{-0.39}$ $(1.17<u<11.7)$	$89\ u^{-0.47}$ $(u>11.7)$
τ_w	$574\ u^{-0.43}$	$422\ u^{-0.39}$ $(0.20<u<1.95)$	$438\ u^{-0.47}$ $(u>1.95)$

The theoretical relations are from section 3.1. It should be noted that the diameter of the wet thermocouple is only known approximately. The observed relations between time constants and wind speed were computed from five measurements at each of the wind speeds of 1, 2, 4, 8 and 16 m s^{-1}. These measurements were carried out with one wet and one dry thermocouple. Other samples of these sensors may have slightly different properties. Moreover the amount of water in the wick affects the time constant. The measurements used for the values in table 1 were carried out 5 seconds after a drop had fallen. About 60 seconds later (just before the next drop) the time constant was up to 15 per cent smaller at high wind speeds. When the water flow had stopped, the value of the time constant dropped to about 60 per cent of its original value, just before the temperature tended to rise due to incomplete wetting.

4.3 Comparison with a ventilated Assman psychrometer

The fast-response psychrometer has been compared with a slow-response ventilated psychrometer of the Assman type (Slob, 1978), mainly with the purpose to see whether or not the psychrometer constant of the fast-response instrument was different from that of the slow-response instrument. Such a difference might be expected on the basis of different shape and size of the wet-bulb sensors (fast-response wet bulb 0.3 mm, slow-response wet bulb about 5 mm. A discussion of this subject is given by Wylie, 1968b). The comparison was carried out outside, under a variety of weather conditions. No differences exceeding 0.2 °C were found, even under low humidity conditions. Therefore, we have no reason to assume a different psychrometer constant for the fast-response instrument than the one for the slow-response psychrometer.

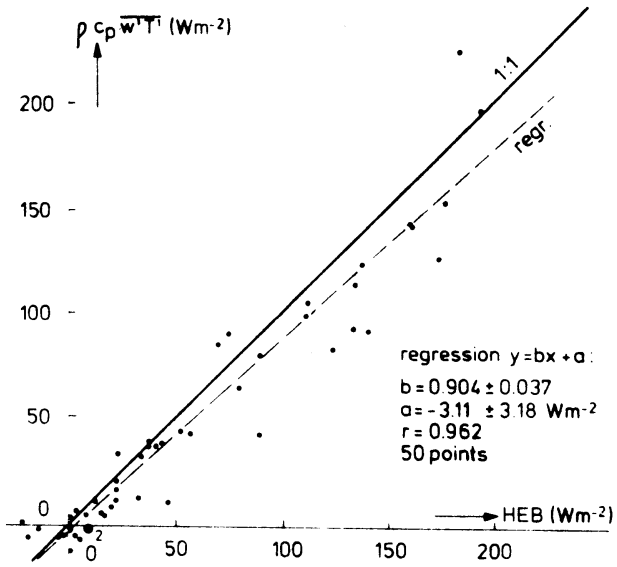

Fig. 4. The sensible heat flux measured at a height of 20 m above grass with a trivane and the fast thermometer ($\rho c_p \overline{w'T'}$), compared with the sensible heat flux measured with the energy budget-Bowen ratio method at a height of about 1 m (HEB). Half-hour averages.

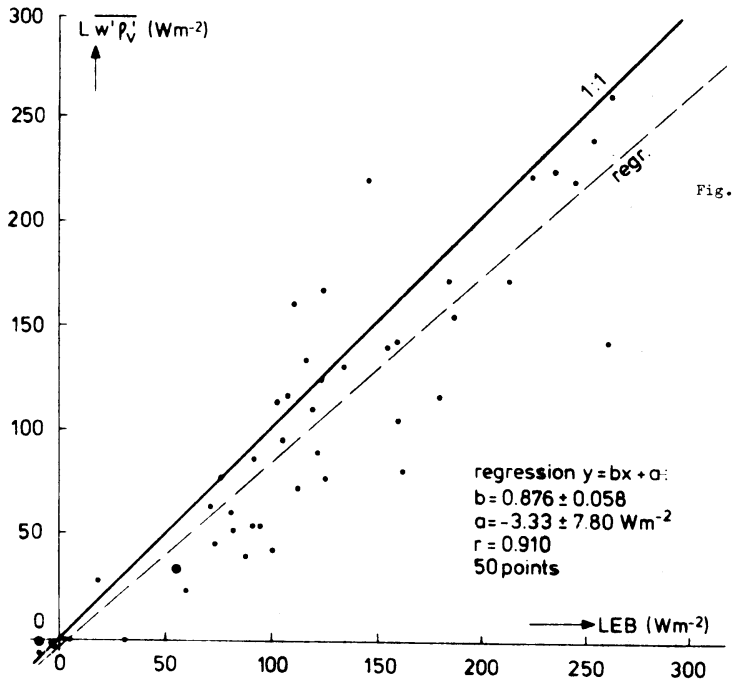

Fig. 5. The latent heat flux measured at a height of 20 m above grass with a trivane and the fast psychrometer ($L\overline{w'\rho_v'}$), compared with the latent heat flux measured with the energy budget-Bowen ratio method at a height of about 1 m (LEB). Half-hour averages.

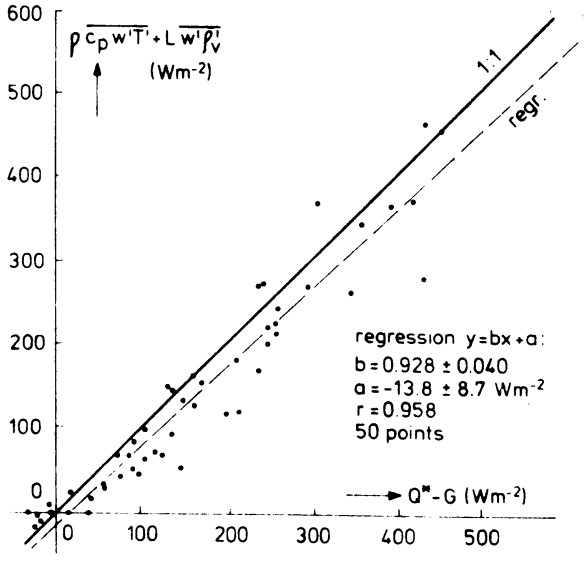

Fig. 6. The flux of enthalpy measured at a height of 20 m with a trivane and the fast psychrometer ($\rho c_p \overline{w'T'} + L\overline{w'\rho_v'}$), compared with the difference of the net radiation and the ground heat flux (Q^*-G). Half-hour averages.

5. Some notes from practice

5.1 Life-span of the sensors

The part of the sensor, which is exposed to the atmosphere, is subject to corrosion. This forms the main limiting factor for the life-span of a sensor. Both the dry-bulb and the wet-bulb sensor are affected. Under normal conditions, the sensor will stand a week's time continuous operation. If the sensor is used intermittently, the mounting and de-mounting procedures may shorten the life-span (shocks, vibrations, etc.). The sensor can stand high wind speeds, but if these are accompanied with heavy rainfall, the thermocouple wire may crack. Hailstones are, of course, disastrous. As a conclusion, the sensor is certainly not fitted for continuous operation over long periods of time; however, it is sturdy enough for special measuring campaigns of several days.

5.2 Measurement of the turbulent fluxes of heat and water vapour at a height of 20 m

Figures 4 and 5 show, as an illustration of flux measurements with the fast psychrometer, the turbulent flux of heat and water vapour at a height of 20 m above the earth's surface, related to the surface fluxes of heat and water vapour. The latter fluxes were determined by the energy budget-Bowen ratio method, the former by correlation of the signals of the psychrometer with those of a trivane (Driedonks et al., 1978; Monna and Driedonks, 1979). The experiments were performed at Cabauw (The Netherlands) on nine days in August and September 1977 under various meteorological conditions. The surface is covered with grass.

In Fig. 6 the sum of the turbulent heat flux and the water vapour flux (the enthalpy flux) is compared with observed values of Q^*-G at the earth's surface, where Q^* is the net radiation and G the ground heat flux. All values are half-hour averages. It is seen that, on the average, the turbulent flux of heat at 20 m is by 10 % lower than that at ground level; for the vapour flux this is 12 % and for the flux of enthalpy 7 %. The scatter of the

points is considerable, especially for the water vapour flux. The decrease of sensible heat flux with height may be attributed to flux divergence in the surface layer (e.g. Wyngaard, 1973). However, the water vapour flux might be more or less constant with height, primarily because entrainment of water vapour near the inversion at the top of the planetary boundary layer results in a strong positive water vapour flux at that place, whereas the same mechanism causes a small negative sensible heat flux (Burk, 1977). These theoretical results seem to be supported by measurements of Druilhet, Guedalia and Fontan (1978).

In calculating the humidity from the dry-bulb and wet-bulb temperatures, we made no account for the phase-shift of the wet-bulb signal at frequencies approaching the inverse of the time constant of the sensor. (The sample frequency was 2 Hz, so the highest contributing frequency is 1 Hz. When we assume a sensor time constant of .3 s, the phase-shift is arctg $\omega\tau = 62^{o}$ at the utmost). The effect of phase of the wet bulb on the observed humidity cannot be calculated without knowledge of the spectral correlation between temperature and humidity. Data on this quantity are given by McBean and Miyake (1972), and, indirectly, by Wesely and Hicks (1978). It appears that both surface boundary conditions and mesoscale conditions affect the magnitude of the correlation. The correlation is high in eddies carrying heat and water vapour vertically over moist surfaces.

6. Conclusions

We have developed a fast thermocouple psychrometer intended for measuring eddy fluxes of heat and water vapour in the atmospheric boundary layer at heights over 20 m. The response times of the wet bulb and the dry bulb were observed experimentally, and agree with calculated values. The wet-bulb response time is 0.3 s at a wind speed of 4 m s^{-1}, which means that the sensor is fast enough for the flux measurements mentioned. The moistening mechanism - a drop of water falling along the vertically mounted

sensor - proved to work reliably in practice, provided that the wick has been wetted in another way before starting the experiments (e.g. with a spraying syringe). The psychrometer constant of the fast psychrometer was found to be the same as for a ventilated (slow) Assman psychrometer.

The temperature of the sensors is slightly (a few tenths of a degree Celsius) affected by radiation; this may influence the measurements of variances (temperature, humidity) under partly broken cloud cover conditions. Furthermore, the falling drops introduce a small additional temperature variance, which may be neglected, however, in most cases. It is strongly recommended to use deionized or destillated water to moisten the wet bulb, because otherwise electrochemical forces may influence the performance of the instrument.

The wet bulb needs no special maintenance. The drops remove dirt from the wick effectively. The life-span of the sensor in operation is of the order of a week, well enough for most measuring campaigns. Several series of measurements with the fast psychrometer have been carried out at a height of 20 and 120 m in the KNMI meteorological tower. A preliminary analysis of part of these measurements confirms the proper functioning of the instrument.

Acknowledgement

The authors express their thanks to Dr. J. Wieringa for his critical reading of the manuscript. Thanks are also due to the technical department of our institute. The eddy flux measurements were carried out under supervision of Messrs A.G.M. Driedonks and F.Th.M. Nieuwstadt.

-o-o-o-

Appendix I. Some properties of Chromel and Alumel

1. Composition

According to Kohlrausch, 1956, the composition is the following:

chromel 89 % Ni + 10 % Cr + 1 % Fe

alumel 94.5 % Ni + 2 % Al + 1 % Si + 2.5 % Mn.

Landolt-Börnstein, 1936, quotes the following composition:

chromel P 90 % Ni + 10 % Cr

alumel 95 % Ni + 2 % Al + 1 % Si + 2 % Mn.

In the International Critical Tables Vol. VI, 1929, we found:

chromel P 90 % Ni + 10 % Cr

alumel 94 % Ni + 2 % Al + 1 % Si + 2.5 % Mn + 0.5 % Fe.

2. Heat capacity

We did not find quotations for the heat capacity of chromel and alumel. As the heat capacities per unit volume ($\rho_c c_{pc}$) of various metals and their alloys do not differ very much, one may assume that the heat capacities of Chromel and Alumel are close to that of their main constituent, Nickel. So we take:

$$\rho_c c_{pc}(\text{chromel, alumel}) \approx \rho_c c_{pc}(\text{nickel}) = 4.0 \times 10^6 \text{ J m}^{-3}\text{K}^{-1}$$

3. Thermal conductivity

Landolt-Börnstein (1936) give the following data:

T =	100	150	200	300	400	500	(^{o}C)
λ(chromel) =	.0454	-	.050	.054	.059	.063	(cal cm^{-1}s^{-1} ^{o}C^{-1})
λ(alumel) =	.070	.072	.076	.083	.091	.098	(cal cm^{-1}s^{-1} ^{o}C^{-1})

We extrapolated these data to 20 ^{o}C, finding:

λ(chromel) = .042 cal cm^{-1}s^{-1} ^{o}C^{-1} = 18 Wm^{-1}K^{-1}

λ(alumel) = .066 cal cm^{-1}s^{-1} ^{o}C^{-1} = 28 Wm^{-1}K^{-1} .

4. Resistance of the thermocouple wires

We measured the resistance of the wires over a known length and found:

chromel wire: 330 Ω/m

alumel wire: 129 Ω/m

The diameters of the wires were measured with a microscope; chromel wire 48 μm, alumel wire 51 μm, with an inaccuracy of about 5 μm. With these data, the electrical resistivity can be calculated; we found:

chromel: 0.60×10^{-6} Ωm (0.71×10^{-6} Ωm)

alumel : 0.26×10^{-6} Ωm (0.33×10^{-6} Ωm)

The values between brackets are quoted by the Intern. Crit. Tables Vol. VI, 1929. The diameters of the wires, calculated from these data, are 52 μm (chromel) and 58 μm (alumel).

-o-o-o-

Appendix II. The internal temperature response of a homogeneous cylinder

We discuss the solution of the differential equation

$$\frac{\partial T}{\partial t} = \kappa \frac{1}{r} \frac{\partial}{\partial r} \left(r \frac{\partial T}{\partial r} \right) \tag{35}$$

with boundary conditions

$$\begin{aligned} T(r,t) &= \Delta T \qquad 0 \leqslant r < R, \quad t=0 \\ T(R,o) &= 0. \end{aligned} \tag{36}$$

We seek solutions of the form:

$$T(r,t) = F(r) \exp \{ - \lambda^2 \kappa t \}. \tag{37}$$

By separation of variables, the function F is found to satisfy the equation:

$$\frac{d^2F}{dr^2} + \frac{1}{r} \frac{dF}{dr} + \lambda^2 F = 0. \tag{38}$$

By substitution of $\xi = \lambda r$ as a new variable, (38) is reduced to the Bessel equation of order zero:

$$\frac{d^2 f(\xi)}{d\xi^2} + \frac{1}{\xi} \frac{df(\xi)}{d\xi} + f(\xi) = 0 \ , \tag{39}$$

where $f(\xi) = F(r)$. The solution of (39) is a linear combination of the zero-order Bessel function $J_o(\xi)$ and the zero-order Neumann function $Y_o(\xi)$. Since the latter function is singular at $\xi = 0$, only the first one is retained:

$$f(\xi) = A J_o(\xi). \tag{40}$$

The second boundary condition leads to:

$$T(R,o) = F(R) = f(\lambda R) = A J_o(\lambda R) = 0 \ , \tag{41}$$

so the admissible values of λ are given by

$$\lambda_n = j_{on}/R \ , \tag{42}$$

where j_{on} is the n^{th} zero of J_o. The general solution of (35) is found by superposition of the special solutions $J_o(\lambda_n r)\ \exp\{-\lambda_n^2 \kappa t\}$:

$$T(r,t) = \sum_{n=1}^{\infty} A_n J_o(\lambda_n r)\ \exp\{-\lambda_n^2 \kappa t\}. \tag{43}$$

The first boundary condition finally leads to the coefficients A_n :

$$T(r,0) = \Delta T = \sum_{n=1}^{\infty} A_n J_o(\lambda_n r)\ . \tag{44}$$

Using the relation of orthogonality

$$\int_o^R J_o(\lambda_m r)\ J_o(\lambda_n r)\ r\ dr = 0 \qquad m \neq n \tag{45}$$

and

$$\int_o^R J_o^2(\lambda_n r)\ r\ dr = \tfrac{1}{2} R^2 J_1^2(\lambda_n R), \tag{46}$$

it follows that

$$A_n = \frac{2\Delta T}{R^2 J_1^2(\lambda_n R)} \int_o^R J_o(\lambda_n r)\ r\ dr = \frac{2\Delta T}{\lambda_n R J_1(\lambda_n R)} \tag{47}$$

because

$$r J_o(r) = \frac{d}{dr}\,(r J_1(r)), \tag{48}$$

(see e.g. Burkill, 1962). Combination of (43), (47), and (42) leads to the final solution:

$$T(r,t) = 2\Delta T \sum_{n=1}^{\infty} \frac{J_o(j_{on} r/R)}{j_{on} J_1(j_{on})} \exp\{-\kappa j_{on}^2\ t/R^2\}. \tag{49}$$

Literature

Burk, S.D., 1977: The moist boundary layer with a higher order turbulence closure model. J. Atmos. Sci. 34, 629-638.

Burkill, J.C., 1962: The theory of ordinary differential equations. Oliver and Boyd, Edinburgh and London.

Driedonks, A.G.M., H. van Dop and W. Kohsiek, 1978: Meteorological observations on the 213 m mast at Cabauw, in the Netherlands. Proc. of the 4th Symposium on Meteorological Observations and Instrumentation of the AMS, Denver, Colo., 41-46.

Druilhet, A., D. Guedalia and J. Fontan, 1978: Caractéristiques de la turbulence dans la couche limite planétaire. Boundary-Layer Meteorol. 15, 147-162.

Dyer, A.J. and F.J. Maher, 1965: The "Evapotron": An instrument for the measurement of eddy fluxes in the lower atmosphere. C.S.I.R.O. Technical Paper No. 15.

International Critical Tables of Numerical Data, Physics, Chemistry and Technology, 1929, New York.

Kohlrausch, F., 1956: Praktische Physik, Band 2, B.G. Teubner, Stuttgart.

Landolt-Börnstein, 1936: Physikalisch-Chemische Tabellen. Springer, Berlin.

McBean, G.A. and M. Miyake, 1972: Turbulent transfer mechanism in the atmospheric surface layer. Quart. J. R. Meteorol. Soc. 98, 383-398.

Monna, W.A.A. and A.G.M. Driedonks, 1979: Experimental Data on the Dynamic Properties of Several Propeller Vanes. J. Appl. Meteorol. 18, 699-702.

Monteith, J.L., 1973: Principles of Environmental Physics. Edward Arnold, London.

Polavarapu, R.J., 1972: Direct measurement of vapour pressure and its fluctuation using fine thermocouples. Quart. J. R. Meteorol. 98, 198-205.

Slob, W.H., 1978: The accuracy of aspiration thermometers. KNMI Scientific Report W.R. 78-1.

Tillman, J.E., 1973: Wet- and dry-bulb thermocouple psychrometry. Atmospheric Technology 2, 77.

van Ulden, A.P., J.G. van der Vliet and J. Wieringa, 1976: Temperature and wind observations at heights from 2 to 200 m at Cabauw in 1973. KNMI Scientific Report W.R. 76-7.

Wesely, M.L. and B.B. Hicks, 1978: High frequency temperature and humidity correlation above a warm wet surface. J. Appl. Meteorol. 17, 123-128.

Wylie, R.G., 1968a: Heat- and vapour-transfer data for calculations relating to psychrometers. C.S.I.R.O. Report PIR-62.

Wylie, R.G., 1968b: An outline of some recent experiments on the psychrometer. C.S.I.R.O. Report PIR-63.

Wylie, R.G., 1968c: Résumé of knowledge of the properties of the psychrometer. C.S.I.R.O. Report PIR-64.

Wyngaard, J.C., 1973: On surface layer turbulence. Workshop on Micrometeorology.(Ed. D.A. Haugen), American Meteorological Society, 101-149.

List of symbols

A	area	m^2
a	absorption coefficient for shortwave radiation	-
C	heat capacity	$J\ K^{-1}$
c_p	specific heat capacity of air	$J\ K^{-1}kg^{-1}$
c_{pc}	specific heat capacity of the dry-bulb sensor	$J\ K^{-1}kg^{-1}$
c_{pw}	specific heat capacity of the wet-bulb sensor	$J\ K^{-1}kg^{-1}$
d	diameter sensor	m
e	distance thermocouple junction - entrance thermocouple wire in housing	m
E	irradiance	$W\ m^{-2}$
J_0, J_1	Bessel function of the order zero, resp. 1	-
j_{on}	n^{th} zero point of J_0	-
k	coefficient of heat conduction of air	$W\ m^{-1}K^{-1}$
L	heat of evaporation of water	$J\ kg^{-1}$
Nu	Nusselt number	-
p	$(2a/\gamma R)^{\frac{1}{2}}$ (dry bulb)	m^{-1}
	$[2a(1+s/\gamma)/\lambda_{eff}R]^{\frac{1}{2}}$ (wet bulb)	m^{-1}
R, R_c, R_w	radius sensor	m
R_e	Reynolds number	-
R_g	electrical resistance galvanic element	Ω
R_{t1}, R_{t2}	electrical resistance thermocouple wires	Ω
r	radial coordinate	m
s	slope of the saturated absolute humidity curve	$kg\ m^{-3}K^{-1}$

T	temperature	^{o}C, K
T_d	dry-bulb temperature	^{o}C, K
T_e	temperature of the thermocouple wire at a certain distance from the junction	^{o}C, K
T_w	wet-bulb temperature	^{o}C, K
t	time	s
U	thermo-electric voltage	μV
U_{g1}, U_{g2}, U_g	galvanic electromotive forces	V
u	wind velocity	$m\ s^{-1}$
V	volume	m^3
x	coordinate along the sensor axis	m
α	heat transfer coefficient	$W\ m^{-2}K^{-1}$
β	water vapour transfer coefficient	$W\ m\ kg^{-1}$
γ	psychrometer coefficient	$kg\ m^{-3}K^{-1}$
λ	coefficient of heat conduction	$W\ m^{-1}K^{-1}$
λ_{eff}	effective heat conduction coefficient wet bulb	$W\ m^{-1}K^{-1}$
κ	thermal diffusivity	m^2s^{-1}
ν	kinematic viscosity of air	m^2s^{-1}
ρ	density of air	$kg\ m^{-3}$
ρ_c	density of the dry-bulb sensor	$kg\ m^{-3}$
ρ_w	density of the wet-bulb sensor	$kg\ m^{-3}$
ρ_v	absolute humidity	$kg\ m^{-3}$
$\rho_{vs}(z)$	saturated absolute hunidity at temperature z	$kg\ m^{-3}$
τ_d	dry-bulb response time	s
$\tau_{int,dry}$	internal dry-bulb time constant	s
$\tau_{int,wet}$	internal wet-bulb time constant	s
τ_w	wet-bulb response time	s